7th European Conference on Industrial Engineering and Operations Management
Augsburg, Germany, July 16-18, 2024
Publisher: IEOM Society International, USA DOI: 10.46254/EU07.20240080
Published: July 16, 2024

Modeling and Investigation of the Effects of Doping-Induced Strain on Boron Diffusion in Thin Film Silicon Solar Cells

Abderrazzak El Boukili
Associate Professor of Applied Mathematics
Al Akhawayn University
Ifrane, Morocco
a.elboukili@aui.ma

Abstract

The goal of this paper is to develop two physically based models to optimize the boron thermal diffusion profiles in novel N-type thin film monocrystalline silicon solar cells. The first model is used to represent the boron doping induced strain. In this model, the strain is position dependent. The second model is used to include the effects of this strain on the boron diffusion coefficient. These models are both applied to investigate and optimize the effects of doping induced strain on boron diffusion. This original investigation will help manufacturers and researchers optimize doping and diffusion parameters and design more robust and highly efficient solar cells. A wide range of doping energies, doses, diffusion times, diffusion temperatures, and different thicknesses of the solar cell films have been tested and qualitatively validated with literature. From this study, we found that the junction depth of the diffused boron dopant is significantly smaller under the effects of the proposed doping induced strain model. The junction depth of the diffused boron with the doping induced strain model is about 71% smaller than that without the doping induced strain.

Keywords

Modeling, strain, diffusion, simulation, solar cells.

1. Introduction

The goal of this paper is to develop two physically based models to help understand and optimize the boron thermal diffusion profiles in novel N-type thin film monocrystalline silicon solar cells. The first model is used to represent the boron doping induced strain. In this model, the strain is position dependent. The second model is used to include the effects of this strain on the boron diffusion coefficient. These models are both original and are applied to investigate and get the taste of the effects of doping induced strain on boron diffusion. As far as we know, this investigation is lacking in the published literature. This original investigation will help manufacturers and researchers optimize doping and diffusion parameters and design more robust and highly efficient thin film silicon solar cells. Thanks to their lower weight and reduced thickness, thin film monocrystalline silicon solar cells (TFMSSCs) are used in applications not suitable for traditional silicon solar cells. For example, thin film silicon solar cells are a better option for vehicles and vertical or curved surfaces. Thin film silicon panels typically cost around $1 to $1.50 per watt. Traditional panels cost around $2.85 per watt. However, TFMSSCs are still less efficient (10% to 18%) compared to traditional thick silicon solar cells (18% to 26%). The aim of this paper is to investigate how to increase the efficiency of TFMSSCs by optimizing the boron dopant thermal diffusion processes at the fabrication level.

1.1 Objectives

The main objectives of this study are as follows. The first objective is to develop an original model to represent the relation between the doping distribution of boron and the induced local strain in the positively dopant region of a thin film silicon solar cell. The second objective is to develop a second model that will include the effects of doping-induced strain in the diffusion coefficient of boron dopant. The third objective

is to apply these innovative models to investigate the effects of doping-induced strain on the junction depth of boron dopant after diffusion. The boron junction depth is the key parameter in this study. The fourth objective is to improve the physical models of pair diffusion used in the open-source two-dimensional process simulator: Suprem-IV (Hansen and Deal 1993). The proposed models are implemented in Suprem-IV.

1.2 Literature Review

The mechanical stress that exists in solar cells is primarily induced by the different technological processes that are used to fabricate solar cells. The challenging problem is that the stress coming from one fabrication process will significantly affect the next fabrication processes and the photovoltaic performance of the solar cell after fabrication. For example, the local stress coming from doping processes will impact the next oxidation and diffusion fabrication processes. On the other hand, some residual stresses will stay in a solar cell even after fabrication and will affect the aging, cracks, lifespan, stability, and efficiency of the solar cell [perovskite solar cells: nano micro letter (Daily et al. 2021), (Rahman et al. 2023). These effects are significant for multijunction or perovskite/silicon tandem solar cells (Kon et al. 2023), (Liu et al. 2022).

The mechanical stress that exists in solar cells during or after fabrication has different sources (Daily et al. 2021). In single or multijunction solar cells, this stress is generated from the material mismatch or thermal mismatch that exists between the different materials that are making up the solar cell (Wu et al. 2021). It can also be generated from the introduced doping atoms in silicon solar cells during doping processes. For example, the boron doping of N-type silicon solar cells is fundamental for the fabrication of the emitter region of the silicon solar cell (Zimbardi et al. 2012), (Ho et al. 2011).

Since boron atoms are smaller than silicon atoms, the lattice spacing between silicon atoms will be modified after doping. This modification of lattice spacing in the bulk silicon will generate a local strain and stress. This strain will significantly influence the diffusion and the activation of boron dopants and defects in the silicon solar cell during the diffusion processes (Liu et al. 2022).

On the other hand, the distribution and the amount of the boron dopants and the defects after diffusion processes will strongly affect the photovoltaic properties of the silicon solar cells (Boyd et al. 2019). For example, too many defects will cause recombination losses of the photogenerated carriers and reduce the optical efficiency of cell.

The originality of this paper is to develop an accurate mathematical model that represents the doping induced strain and apply it to quantitively investigate the positive and negative effects of this induced strain on the boron diffusion and activation in the state-of-the-art textured silicon solar cells. The proposed strain model is applied to calculate the diffusion coefficient of boron under the impact of different doping and diffusion conditions.

According to the published literature, the impact caused by doping induced strain or stress on boron diffusion in silicon solar cells has not yet been investigated theoretically or experimentally. The study in this paper represents an initial attempt to the first investigation of this impact.

From recent literature, most of the published research work has been focused on the study of the negative effects of stress and strain on the solar cells after fabrication and not during fabrication.

The negative effects of residual stress on the environmental stability, wrinkling, and fracture of perovskite thin film solar cells have been discussed in (Kong et al. 2023), (Wang et al. 2023). Key sources of the instabilities in perovskite solar cells are ion migration and defects that are tied to high residual stresses that exist in perovskite materials after fabrication. Mitigation strategies for these stresses have been highlighted in (Daily et al. 2019). The effect of high compressive stress on the failure and delamination of perovskite layers has been studied in (Daily et al. 2021), (Bush et al. 2018), (Kim et al. 2021). Moreover, the impact of the strain in the perovskite layer on the neighboring layers has been discussed in (Bush et al. 2018).

The peeling-of or wrinkling in perovskite/silicon tandem solar cells due to sputtering induced stress has been studied and reported in (Liu et al. 2022). The use of encapsulation techniques to help mitigate stress induced harm to the perovskite solar cells has been highlighted in (Boyd et al. 2019). In general, even moderate stress can cause dislocations or defects at the interface, leading to recombination losses of photogenerated carriers. The modulation of

strain in perovskite/silicon tandem solar cells by adding adenosine triphosphate has been reported in (Wang et al. 2022).

Different substrates cause different levels of lattice mismatching between the perovskite and the substrates, leading to different stress and bandgap in perovskite cells. The work reported in (Cheng et al. 2019) found that the photoluminescence peak of the perovskite film on silicon substrate exhibited blue shift compared with that on glass substrate.

On the other hand, there has been a great deal of research work devoted to the study of the effects of stress, due to material or thermal mismatch, on the dopant diffusion behavior in CMOS transistors (Fang et al. 2021), (Zeng et al. 2019). However, even for CMOS transistors, no study has been done about the effects of doping induced stress on dopant diffusion. In this research paper, we are focusing on the investigation of the effects of doping induced strain and stress on the dopant diffusion in thin film silicon solar cells and not in CMOS transistors.

It is well recognized that the key parameters for silicon solar cells, such as short circuit current, open circuit voltage, recombination losses, spectral losses, and photovoltaic efficiency are all strongly dependent on dopant diffusion details. Thus, it is crucial to examine strain-dependent dopant diffusion for the state-of-the-art silicon solar cells under doping induced mechanical strain.

In this paper, we present an original and position dependent doping-induced strain model. Then, we include this model in the diffusion coefficient model of boron dopant. The boron diffusion equations are then modified and incorporated into a two-dimensional process simulation environment. We conducted extensive numerical experiments and validations under different doping and diffusion conditions in a sample N-type monocrystalline silicon solar cell.

This paper is organized as follows. Section 2 outlines the detailed derivation of the doping-induced strain model. This proposed model is original and accurate. Section 3 introduces the development of the second proposed model for strain-dependent boron diffusion. This section explains how the first model is included in the diffusion coefficient of boron.
Section 4 presents and analyzes the numerical results obtained from the application of the two proposed models. A qualitative comparison of the obtained results with literature is presented as well. Section 5 summarizes the concluding thoughts.

2. Doping-Induced Strain Model

The efficiency of a silicon solar cell depends mainly on the fabrications processes such as texturing, doping, oxidation, and diffusion. The first originality in this paper is the development of a mathematical model to represent the strain induced by doping processes. When dopants are introduced into a silicon solar cell, the mechanical state of the silicon solar cell will be modified. The dopants could substitute for the silicon positions in the solar cell. Then, silicon atoms are displaced into interstitial positions forming self-extended point-defects in the crystal lattice of the cell. In general, different dopants have different atomic sizes and therefore have different mechanical behavior in silicon crystal of the cell. Different defects introduced by doping such as point-defects, precipitates, clusters, or dislocation loops will also impact the optical and mechanical properties of the silicon solar cell and cause local strains.

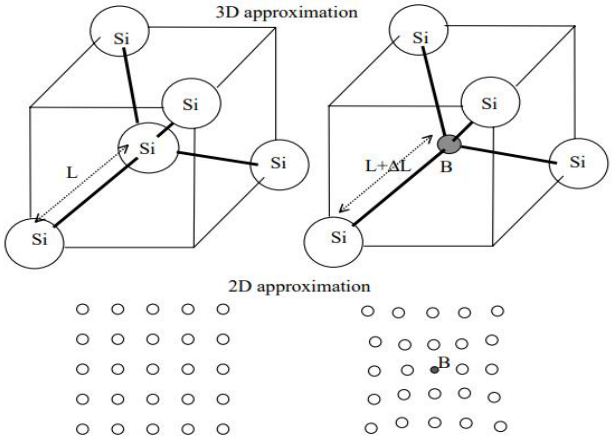

Figure 1. Lattice deformation due to doping.

The boron dopant is well known as a substitutional dopant (Hansen et al. 1993). Its atomic size is smaller than that of silicon. When it is in a substitutional site, lattice contraction results due to its smaller size, see Figure 1. Each boron dopant atom will create an atomically localized strain in silicon as graphically illustrated by Figure 1.

When the concentrations of boron dopant in a silicon solar cell are high, the local atomic strains add up significantly and produce a larger localized region of strain in the boron doped region of the silicon solar cell under hand.

The non-boron doped silicon region will resist the diffused boron layer from contracting and thus result in a tensile strain. This effect has been demonstrated in silicon micro-machining applications (Wang et al. 2022), (Cheng et al. 2019), where boron-doped cantilevers have shown bending due to strain induced by the boron dopant atoms.

Different densitometric studies have been done with boron doped silicon crystals. The dependence of the silicon lattice constant on boron dopant concentration has been measured by Horn (Horn et al. 1955). From the measurements of Horn, the induced hydrostatic strain (Δa/a) was extracted and given as a function of the average of the boron dopant concentration $C_B(x,y), \forall (x,y) \in \Omega$. Here, Ω represents the silicon solar cell we are simulating. A sample is shown in Figure 4. The boron induced strain model, we are proposing in this paper, is a simple linear model with respect to the dopant concentration $C_B(x,y)$. It is given as follows:

$$\varepsilon_{xx}(C_B(x,y)) = \varepsilon_{xx}(x,y) = \varepsilon_{yy}(x,y) = AC_B(x,y) + B \quad (1)$$

A, B are constants.

We have taken the constants A and B as follows:

$$A = \frac{c}{a_{Si} N_{Si}} \times 100; B = 0$$

where a_{Si} is the unstrained silicon lattice constant (5.4295 Angstrom at 25°C), N_{Si} is the density of Si atoms (5.02e22/cm3), c is a constant, and $C_B(x,y)$ is the boron dopant concentration at any point (x, y) in the solar cell. The functions $\varepsilon_{xx}(x,y)$ and $\varepsilon_{yy}(x,y)$ represent the local normal strains respectively. The local strain $\varepsilon_{xx}(x,y)$ represents the deformation of the solar cell, due to boron doping, along x-axis and normal to the yz-plane. The local strain $\varepsilon_{yy}(x,y)$ represents the deformation of the solar cell, due to doping, along y-axis and normal to the xz-plane. The shear strain ε_{xy} is ignored in this study.

The value of the constant c has been taken from the empirical model introduced by Horn (Horn 1955). In the empirical model of Horn, $C_B(x,y)$ is replaced by the average boron dopant concentration $\overline{C_B}(x,y)$. In our proposed model, the boron dopant concentration, $C_B(x,y)$, is calculated accurately and analytically using Dual-Person IV model. A detailed description of the calculation of the function $C_B(x,y)$ is given in our previous publication (El Boukili 2019).

3. Strain-Dependent Diffusion Model

The second originality in this paper is to develop a physically based model that includes the doping induced strain given in the Equation (1) into the boron diffusion coefficient, D_{AI}, and the paired boron diffusion equation given below in the Equation (2).

The optical efficiency of any silicon solar cell depends strongly on the thermal diffusion process of the implanted n-dopant or p-dopant ions as boron dopant ions. This thermal diffusion process is needed to activate the implanted dopant ions (A) and to repair the damage caused by the implantation process. The implantation damage is represented by the existence of point-defect ions. The point-defect ions are represented by interstitial ions (I) and vacancy ions

(V). The thermal diffusion of all these charged ions A, I, and V is due to their unequal concentrations, internal electric field, and temperature (El Boukili 2019).

The derivation of the coupled diffusion equations for the ions A, I, and V is based on the continuum theory using Fick's laws and the atomistic theory (Hansen et al. 1993). The advanced models of the dopant ions diffusion are based on the idea of pair-diffusion. This means, most of the dopant ions, A, can't diffuse on their own. However, they need the neighboring point-defects I and V as diffusion vehicles as shown in Figure 2.

When a binding energy between a dopant impurity, A, and a neighboring defect I or V is not weak, the impurity A and the point defect I or V will move as a pair impurity-defect AI or AV until they get separated by recombination or other factors. The pair-diffusion mechanism is shown in Figure 3.

Some dopants will diffuse with vacancies only, some with interstitials only and some could diffuse with both. For example, boron dopant ions are known to diffuse with interstitials. Phosphorus will diffuse with interstitials at low doping and with interstitials and vacancies at high doping (Hansen et al. 1993).

Let $C_T(x,y,t,T)$ be the total concentration of all the ionized dopants after t seconds of thermal diffusion under the temperature T at the point (x, y) in the solar cell. Let $C_{TI}(x,y,t,T)$, and $C_{TV}(x,y,t,T)$ be the total concentrations of interstitials and vacancies, respectively. We have:

$$C_T = C_A + C_{AI} + C_{AV}$$

$$C_{TI} = C_I + C_{AI}, \quad C_{TV} = C_V + C_{AV}$$

Where $C_A(x,y,t,T)$, $C_I(x,y,t,T)$, and $C_V(x,y,t,T)$ are the concentrations of the unpaired dopants, interstitials, and vacancies, respectively. The $C_{AI}(x,y,t,T)$, and $C_{AV}(x,y,t,T)$ are the concentrations of the paired dopants (A) or the paired interstitials (I) or the paired vacancies (V). The diffusion model we are solving involves 6 coupled partial differential equations of second order whose unknowns are: the electrostatic potential $\varphi(x,y,T)$ and the 5 coupled concentrations: $C_A(x,y,t,T), C_I(x,y,t,T), C_V(x,y,t,T)$ and $C_{AI}(x,y,t,T), C_{AV}(x,y,t,T)$. To illustrate the strain-dependent diffusion model we are proposing, we present only one diffusion equation for boron dopant. This equation is given as follows:

$$\frac{\partial C_{AI}(x,y,t,T)}{\partial t} = -div(J_{AI}) + R_{AI} \qquad (2)$$

Where:

$$J_{AI} = D_{AI} C_{AI} \nabla \ln(C_{AI} \frac{n}{n_i})$$

The terms: R_{AI}, n, n_i are described in our previous work (El Boukili 2019).

The term: D_{AI} represents the diffusion coefficient of boron ions without strain. This is the term we want to modify to include the effects of doping induced strain on the paired diffusion of boron dopant ions. To include the effects of strain on the paired diffusion of boron dopant, we use Arrhenius form as follows:

$$D_{SAI} = D_{AI} \exp(-\varepsilon_t(x,y) AE) \qquad (3)$$

Where D_{SAI} is the diffusion coefficient of boron dopant ions under strain. D_{AI} is the diffusion coefficient of boron dopant ions without strain. EA is the activation energy per strain. The term $\varepsilon_t(x,y)$ is the total local strain given by:

$\varepsilon_t(x,y) = \varepsilon_{xx}(x,y) + \varepsilon_{yy}(x,y)$.

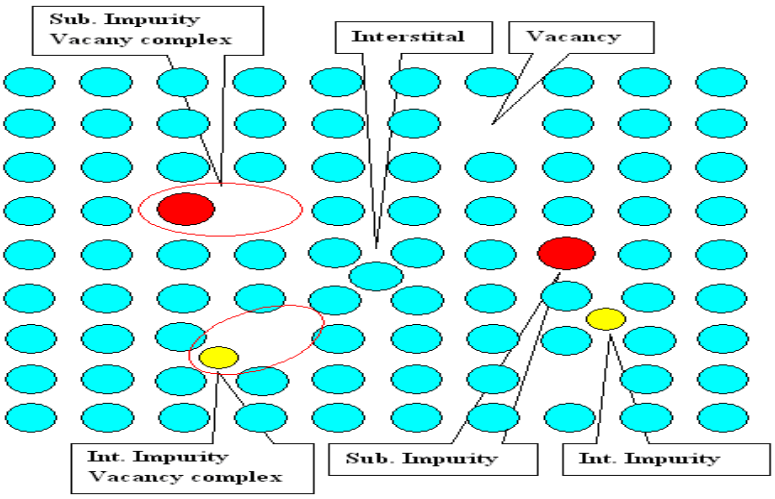

Figure 2. Pair-Diffusion mechanisms.

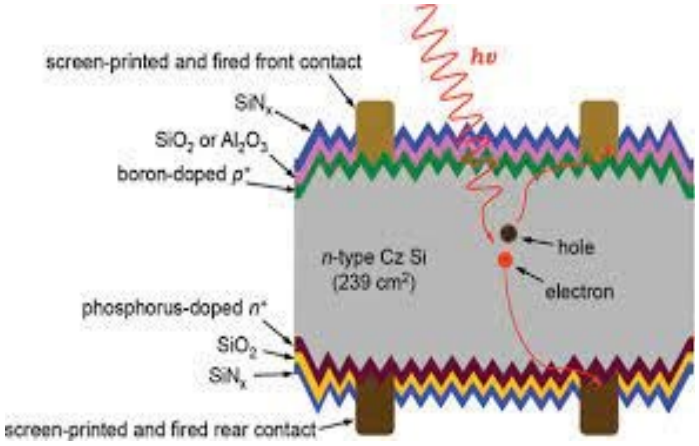

Figure 3. Textured N-type traditional silicon solar cell.

4. Results and Discussion

4.1 Numerical and Graphical Results

The sample structure we are using to test and validate the proposed models is an N-type TFMSSCs (001), textured with 2 identical pyramids of faces (111) as shown in Figure 4. We have tested the models for a range of implantation doses going from 1.0e15 to 4e15 atoms per square centimeter and a range of diffusion temperatures going from 800°C to 1100°C.

Figure 5 shows the simulated 2D contour lines of boron doping profile after diffusion with the proposed doping induced strain model. This result is qualitatively in a good agreement with measurements and simulations found in

literature (Ma et al. 2014). Figure 6 shows the simulated 2D contour lines of boron doping profile after diffusion without the proposed doping induced strain model. This result is qualitatively in a good agreement with measurements and simulations found in literature (Ma et al. 2014).

Figure 7 shows a vertical cut at x=0.5 microns of the boron dopant after diffusion with the effect of doping induced strain when t=20mn, T=900°C, and the implantation dose is 2e15 atoms per square centimeter. Figure 8 shows a horizontal cut at y=1 microns of the boron dopant after diffusion with the effect of the doping induced strain when t=20mn, T=900°C, and the implantation dose is 2e15 atoms per square centimeter. We consider the boron doping induced strain to be compressive since the boron atoms are smaller than the silicon atoms.

Figure 9 shows a vertical cut at x=0.5 microns of the boron dopant after diffusion without the effect of doping induced strain when t=20mn, T=900°C, and the implantation dose is 2e15 atoms per square centimeter. Figure 8 shows a horizontal cut at y=1 microns of the boron dopant after diffusion without the effect of the doping induced strain when t=20mn, T=900°C, and the implantation dose is 2e15 atoms per square centimeter.

From Figure 9, we see that the junction depth is about 1.12 microns. However, we see from Figure 7 that the junction depth is about 0.8 microns. This comparison explains clearly that the compressive boron doping induced strain significantly decreases the boron junction depth. Then, the boron diffusion is clearly retarded by the compressive strain coming from doping atoms. The efficiency of the solar cell depends strongly on the junction depth of the dopants.

Figures 8 and 10 show a lateral cut, at y=1 microns, of the diffused boron profiles with and without doping induced strain. From these Figures 8 and 10, we see clearly that the doping induced strain significantly affects the lateral distribution of the boron dopant as well. It does show that the junction depth depends also on the horizontal dimension (x). This is explained by the effects of texturing. The junction depth is smaller below the valleys between the pyramids compared to the junction depth below the tips of the pyramids. This is a great finding from the proposed models.

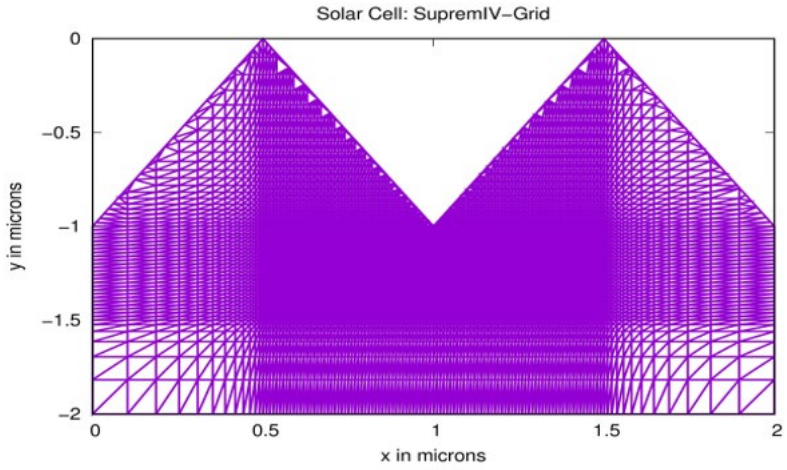

Figure 4. Sample textured solar cell with 2 pyramids using Suprem-IV meshing (Hansen et al. 1993).

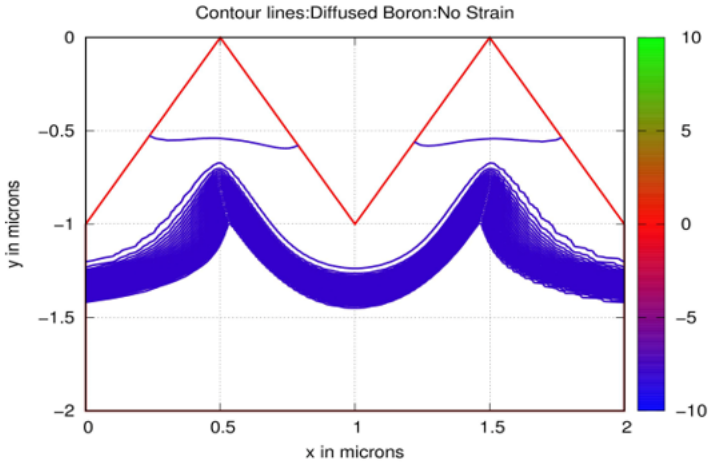

Figure 5. Simulated 2D Contour lines of Boron profile after diffusion when t=20mn, T=900°C, and no doping-induced strain model.

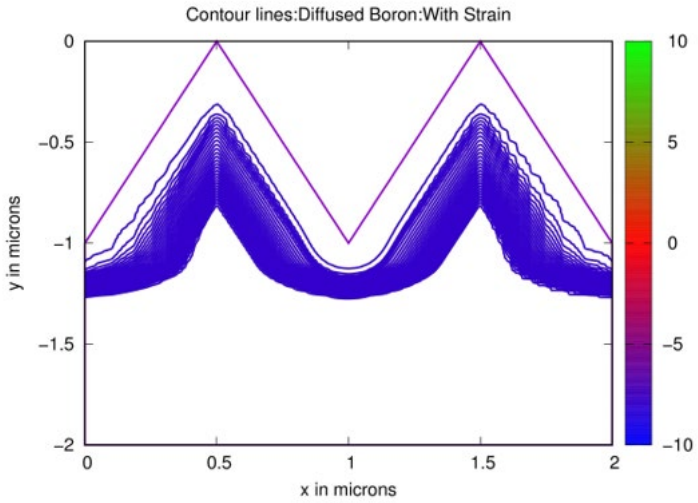

Figure 6. Simulated 2D Contour lines of Boron profile after diffusion when t=20mn, T=900°C, and with doping-induced strain model.

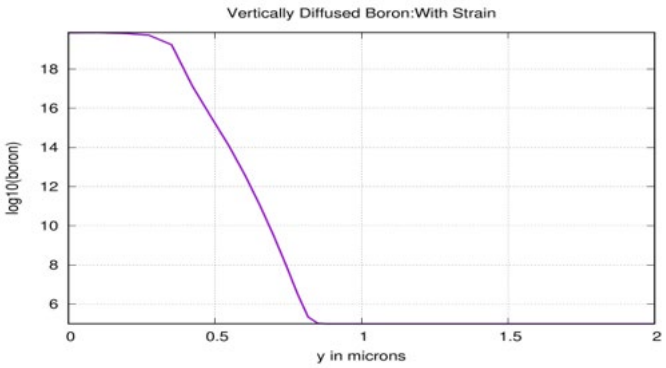

Figure 7. Vertical cut, at x=0.5 um, of Boron profile after diffusion when t=20mn, T=900°C, and with doping-induced strain model.

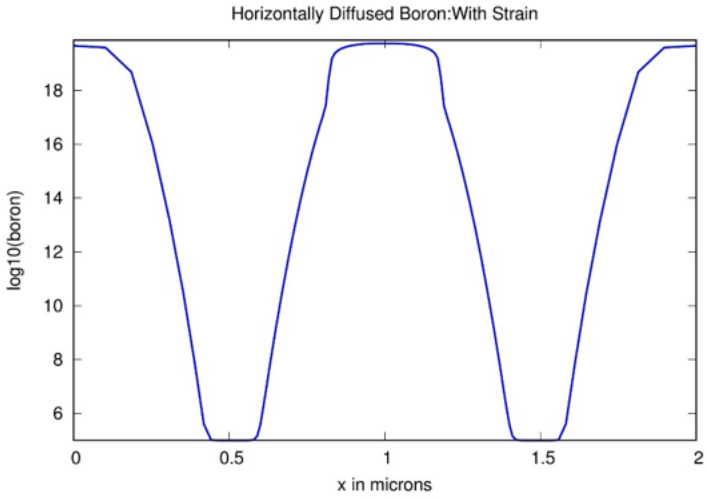

Figure 8. Vertical cut, at x=0.5 um, of Boron profile after diffusion when t=20mn, T=900°C, and with doping-induced strain model.

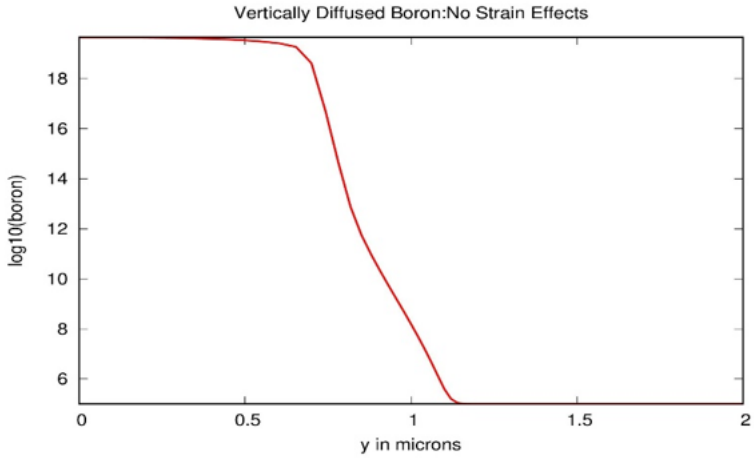

Figure 9. Vertical cut, at x=0.5 um , of Boron doping profile after diffusion when t=20mn, T=900°C, and without doping-induced strain model.

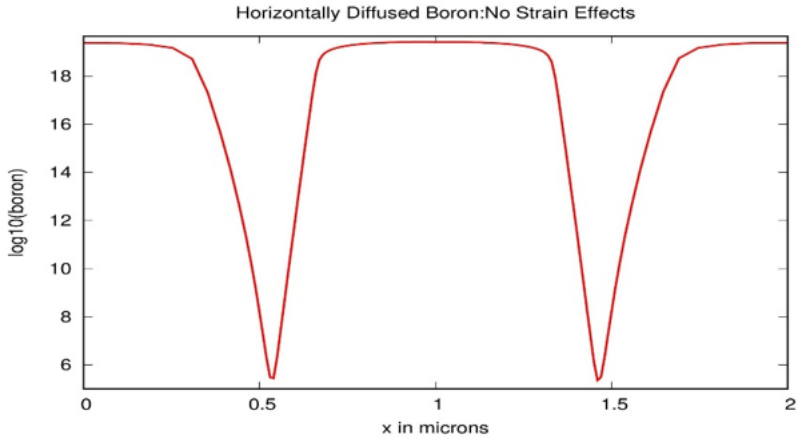

Figure 10. Horizontal cut, at y=1 um, of Boron doping profile after diffusion when t=20mn, T=900°C, and with doping-induced strain model.

4.2 Proposed Improvements

In this study we are considering the doping induced local strain, $\varepsilon_{xx}(x,y)$, along x-direction to be uniaxial and identical to the strain, $\varepsilon_{yy}(x,y)$, along y-direction at a given point (x, y) on solar cell . This means, we are taking: $\varepsilon_{xx}(x,y) = \varepsilon_{yy}(x,y)$. In the future work we are going to consider in the proposed model (1) the difference that may exist between the lattice constant of silicon in x and y directions. We think this idea will improve the accuracy of the proposed model. We are also planning to improve the proposed model (1) by including the effects of the diffusion temperatures, T, on the doping-induced strains, $\varepsilon_{xx}(x,y)$ and $\varepsilon_{yy}(x,y)$.

5.4 Validation

We have tested and validated the proposed models using different doping and diffusion parameters. We have tested different values of implantation doses from 1e15 to 4e15 and different values of diffusion temperatures from T=800°C to T=1100°C. The diffusion time was fixed to 20mn. The obtained results in Figures 5 to 9 have been compared and validated qualitatively with experiments and simulations results found in the published literature for similar structures (Ma et al. 2014). Ma et al. (2014) have studied experimentally and numerically different diffusion and oxidation methods of boron in textured solar cells. Ma et al. (2014) did not study the effects of strain on diffusion as we are doing in this paper. To the best of our knowledge no study has been done about the effects of doping-induced strain on the diffusion of dopants in published literature in the areas of solar cells or even CMOS transistors.

6. Conclusion

We have shown that the junction depth of the diffused boron dopant has been reduced by about 71% under the effects of the boron doping induced strain. Then, the diffusion of boron under this compressive strain is significantly retarded which will impact deeply the open circuit voltage and the short circuit current of the solar cell. In the future work, we will investigate the output power and the efficiency of silicon solar cells under doping induced strain.

References

Hansen, S. and Deal, M., *Two-dimensional process simulation for silicon and Gallium arsenide,* Suprem IV User's Manual, Stanford University, USA, 1993.

Kong, L., Zhijie, W., Shengchum, Q. and Liming, D., Stress and strain in Perovskite/Silicon tandem solar cells, *Nano-Micro Letter, 2023.*

Dailey, M., Li, Y.N. and Printz, A.D., Residual film stresses in perovskite solar cells: origins, effects, and mitigation strategies. *ACS Omega 6(45), pp. 30214–30223, 2021.*

Bush, K.A., Rolston, N., Gold-Parker, A., Manzoor, S. and Hausele, J., Controlling thin-film stress and wrinkling during perovskite film formation*, ACS Energy Lett. 3(6), pp. 1225– 1232, 2018.*

Kim, S.G., Kim, J.H., Ramming, P., Zhong, Y. and Schotz, K., How antisolvent miscibility affects perovskite film wrinkling and photovoltaic properties, *Nat. Commun. 12(1), 1554, 2021.*

Liu, K., Chen, B., Yu, Z.S.J., Wu, Y.L. and Huang, Z.T., Reducing sputter induced stress and damage for efficient perovskite/ silicon tandem solar cells, *J. Mater. Chem. A 10(3), pp. 1343– 1349, 2022.*

Boyd, C.C., Cheacharoen, R., Leijtens, T. and McGehee, M.D., Understanding degradation mechanisms and improving stability of perovskite photovoltaics, *Chem. Rev. 119(5), 2019, pp. 3418–3451, 2019.*

Wang, L.N., Song, Q., Pei, Z., Chen, Y.H and Dou, J., Strain modulation for light-stable n-i-p perovskite/silicon tandem solar cells, *Adv. Mater. 34(26), 01315, 2022.*

El Boukili, A., Modeling and analysis of the impact of texturing angles on doping profiles in ion implanted N-Type solar cells, *Proceedings of the 7th International Workshop on Simulation for Energy, Sustainable Development and Environment (SESDE 2019), pp. 1-6, Lisbon, Portugal, 2019.*

Ma, F.I., Duttagupta, S., Devappa, K.S., Meng, L., Samudra, G.S., Hoex, B. and Peters, S.M., Two-dimensional numerical simulation of boron diffusion for pyramidally textured silicon, *Journal of Applied Physics, 116, pp. 1-8, 2014.*

Horn, H.F., Densitometric and electrical investigation of boron in silicon, *Physical Review, vol. 97, pp. 1521-1525, 1955.*

Wu, J.P., Liu, S.C., Li, Z.B., Wang, S. and Xue, D.J., Strain in perovskite solar cells: origins, impacts and regulation, *Natl. Sci. Rev. 8(8), 2021.*

Zhang, H. and Park, N.G., Strain control to stabilize perovskite solar cells, *Angew. Chem. Int. Ed. 61(48), e202212268, 2022.*

Yang, B.W., Bogachuk, D., Suo, J.J., Wagner, L. and Kim, H., Strain effects on halide perovskite solar cells, *Chem. Soc. Rev. 51(17), pp. 7509–7530, 2022.*

Liu, K., Chen, B., Yu, Z.S., Wu, Y.L. and Huang, Z.T., Reducing sputter induced stress and damage for efficient perovskite/ silicon tandem solar cells, *J. Mater. Chem. A 10(3), pp. 343–1349, 2022.*

Chen, B., Yu, Z.S., Liu, K., Zheng, X.P. and Liu, Y., Grain engineering for perovskite/silicon monolithic tandem solar cells with efficiency of 25.4%, *Joule 3(1), pp. 177–190, 2019.*

Fang, Z., Zeng, Q., Zuo, C., Zhang, L. and Xiao, H., Perovskite based tandem solar cells, *Sci. Bull. 66(6), pp. 621–636, 2021.*

Zeng, Q., Liu, L., Xiao, Z., Liu, F. and Hua, Y., A two-terminal all-inorganic perovskite/organic tandem solar cell, *Sci. Bull. 64(13), 2019, pp. 885–887, 2019.*

Biography

Abderrazzak El Boukili is an Associate Professor of Applied Mathematics at Al Akhawayn University in Ifrane, Morocco. He earned B.S. in Applied Mathematics from Picardie University, Amiens, France and a M.S. in Applied Mathematics from the University of Piere et Marie Curie (Paris 6), Paris, France and an Industrial PhD in Applied Mathematics to Heterojunction Bipolar Transistors used as Amplifiers in Mobile Telephones from the University of Piere et Marie Curie (Paris 6), Paris, France. During his industrial PhD, he worked on an industrial project which was under a joined collaboration between the University of Piere et Marie Curie (Paris 6), Paris, France and National Institute of Research in Computer Science and Automatics, Versailles, France and National Center of Telecommunication Studies, Bagneux, France. He worked as Senior Software Developer in Silvaco Software Inc., Santa Clara, USA and in Crosslight Software Inc., Vancouver, British Columbia, Canada. He worked as Associate Professor of Applied Mathematics at Al Akhawayn University in Ifrane, Morocco since August 2008 till now.